May 12, 2015

2013 IAPT Research Grant – Nicolás García

Study Report

Amaryllidaceae tribe Hippeastreae, a Neotropical group of asparagoid lilies (i.e., Asparagales), constitutes a good model to address reticulate evolution from several perspectives. First, this group has been hypothesized to have undergone ancient hybridization(s) prior to its major radiation (Meerow 2010). Second, allopoplyploidy has been likely involved in the diversification of Hippeastreae, especially within *Habranthus* and *Zephyranthes* (e.g., Flory 1977; Greizerstein and Naranjo 1987). And third, Hippeastreae show extensive variation in chromosome numbers (Flory 1977; Meerow and Snijman 1998; García et al. 2014), which, coupled with the relatively large chromosomes of Amaryllidaceae in general, makes it ideal to address chromosome number dynamics in the context of reticulate evolution. Furthermore, the taxonomy of this group has been historically problematic, and generic limits have remained ambiguous, due to the lack of a clear phylogenetic framework and unequivocal morphological characters (e.g. Hutchinson 1959; Traub 1963; Meerow and Snijman 1998).

In my doctoral research, three major components of systematic biology – DNA sequences, chromosomes, and morphology – were investigated to develop a phylogenetic classification of Amaryllidaceae tribe Hippeastreae. An emphasis was made on inferring the group's phylogeny with the ultimate goal of translating this pattern into a classification at the genus level. A first step towards exploring the phylogeny of Hippeastreae was to increase the taxon sampling for ITS in relation to previous studies and obtain a well-resolved tree derived from multiple chloroplast DNA (cpDNA) markers (i.e., *trnL-F, ndhF,* 3'*ycf1*). These molecular markers provided strong support for two major clades within Hippeastreae that were formalized by García et al. (2014) as subtribes: Traubiinae and Hippeastrinae. Supporting Meerow's hypothesis of deep reticulation, widespread cytonuclear discordance was detected in Hippeastrinae, while Traubiinae showed a tree-like pattern of evolution, consistent with an apparent lack of allopolyploidy.

The IAPT Research Grant directly supported the study of chromosome evolution in Hippeastreae through the analysis of copy number variation and location of 5S and 45S rDNA FISH markers (see Figures 4-1 to 4-5 in Chapter 4, attached). The extensive copy number variation of these markers was not easy to interpret, and it is probably not linearly related to ploidy, as suggested in similar studies (see Weiss-Schneeweiss and Schneeweiss 2013). However, the nrDNA constellations of core *Rhodophiala* and *Phycella-Placea* were interpreted as likely synapomorphies for those clades.

Additionally, probabilistic models of chromosome number evolution in ChromEvol (Mayrose et al. 2010; Glick and Mayrose 2014) were used to infer ancestral haploid chromosome numbers of Hippeastreae and Hippeastrinae, and the relative importance of various mechanisms of transitions in chromosome number throughout the ITS and cpDNA gene trees, and diploid species trees of Hippeastreae. The ancestral number for Hippeastreae remains equivocal given the sampling of outgroups in the trees used. Three most likely ancestral chromosome numbers were inferred for Hippeastrinae depending on the tree used, $2n = 12$, 18, and 22. Overall, more losses than gains were inferred to explain chromosome number variation, consistent with the traditional hypothesis of $2n = 22$ as the most likely ancestral number for Amaryllidaceae (Flory 1977; Meerow and Snijman 1998; Naranjo and Poggio 2000) and, likewise, for Hippeastrinae.

Finally, an explicit hypothesis of phylogenetic relationships and morphological evolution was postulated for Hippeastreae. This scenario was translated into a classification at the generic level, which accommodated this clade's network-like pattern of diploid evolution through the adoption of a synchronic definition of monophyly that focuses on extant species in order to delimit clades (e.g., Mishler 2010; Podani 2010). In addition, I attempted to maximize several secondary criteria of ranked phylogenetic classification, the most relevant being support for monophyly, diagnosibility, and nomenclatural stability (Backlund and Bremer 1998). The proposed taxonomy for Hippeastreae consists of 10 genera that are treated in terms of their nomenclature, morphology, composition, and distribution; additionally, a key to identify the genera was developed.

Literature Cited

Backlund, A. and K. Bremer. 1998. To be or not to be. Principles of classification and monotypic plant families. *Taxon* 47: 391–400.

García, N., A. W. Meerow, D. E. Soltis, and P. S. Soltis. 2014. Testing deep reticulate evolution in Amaryllidaceae tribe Hippeastreae (Asparagales) with ITS and chloroplast sequence data. *Systematic Botany* 39: 75–89.

Glick, L. and I. Mayrose. 2014. ChromEvol: assessing the pattern of chromosome number evolution and the inference of polyploidy along a phylogeny. *Molecular Biology and Evolution* 31: 1914–1922.

Greizerstein, E. J. and C. A. Naranjo. 1987. Estudios cromosómicos en especies de *Zephyranthes* (Amaryllidaceae). *Darwiniana* 28: 169–186.

Flory, W. S. 1977. Overview of chromosomal evolution in the Amaryllidaceae. *Nucleus* 20: 70–88.

Hutchinson, J. 1959. *The families of flowering plants. Vol. II. Monocotyledons. 2nd edition.* Oxford: Clarendon Press.

Mayrose, I., M. S. Barker, S. P. Otto. 2010. Probabilistic models of chromosome number evolution and the inference of polyploidy. *Systematic Biology* 59: 132–144.

Meerow, A. W. 2010. Convergence or reticulation? Mosaic evolution in the canalized American Amaryllidaceae. Pp. 145–168 in *Diversity, phylogeny, and evolution in the monocotyledons*, eds. O. Seberg, G. Petersen, A. S. Barfod and J. I. Davis. Aarhus: Aarhus University Press.

Meerow, A. W. and D. A. Snijman. 1998. Amaryllidaceae. Pp. 83–110 in *Families and genera of vascular plants, volume 3,* ed. K. Kubitzki. Berlin: Springer-Verlag.

Mishler, B. D. 2010. Species are not uniquely real biological entities. Pp. 110–122 in *Contemporary Debates in Philosophy of Biology*, eds. F. J. Ayala and R. Arp. Oxford: Wiley-Blackwell.

Naranjo, C. A. and L. Poggio. 2000. Karyotypes of five *Rhodophiala* species (Amaryllidaceae). *Boletín de la Sociedad Argentina de Botánica* 35: 335–343.

Podani, J. 2010. Monophyly and paraphyly: a discourse without end?. *Taxon* 59: 1011–1015.

Traub, H. P. 1963. *Genera of the Amaryllidaceae.* La Jolla: American Plant Life Society.

Weiss-Schneeweiss, H. and G. M. Schneeweiss. 2013. Karyotype diversity and evolutionary trends in angiosperms. Pp. 209–230 in *Plant genome diversity, Volume 2: Physical structure, behaviour and evolution of plant genomes*, eds. I. J. Leitch, J. Greilhuber, J. Doležel, and J. F. Wendel. Wien: Springer-Verlag.

SYSTEMATICS AND EVOLUTION OF AMARYLLIDACEAE TRIBE HIPPEASTREAE (ASPARAGALES)

By

NICOLÁS GARCÍA BERGUECIO

A DISSERTATION PRESENTED TO THE GRADUATE SCHOOL
OF THE UNIVERSITY OF FLORIDA IN PARTIAL FULFILLMENT
OF THE REQUIREMENTS FOR THE DEGREE OF
DOCTOR OF PHILOSOPHY

UNIVERSITY OF FLORIDA

2015

CHAPTER 4

CYTOGENETICS OF HIPPEASTREAE: INSIGHTS FROM FISH OF NUCLEAR RIBOSOMAL DNA AND PROBABILISTIC MODELS OF CHROMOSOME NUMBER EVOLUTION

Comparative cytogenetic analyses have undergone a revival, especially when coupled with a robust phylogenetic framework (e.g., Lim et al. 2006; Mlinarec et al. 2011; Chacón et al. 2012; Gan et al. 2013; Sousa et al. 2014). Amaryllidaceae s. s. constitute an ideal group for cytological study because of their large chromosomes and previous inferences of chromosomal evolution (Flory 1977). Previous comparative analyses of karyotypes and chromosome evolution within Amaryllidaceae have highlighted the importance of chromosome number variation via fusions/fissions (i.e., Robertsonian exchanges) and polyploidy (e.g., Shi et al. 2006; Chang et al. 2009); however, little work has been done in this family using modern cytogenetic methods such as fluorescence *in situ* hybridization (FISH). Under a comparative framework, this methodology has detected chromosomal rearrangements (translocations, inversions, deletions) and directions of chromosomal evolution in other groups (e.g., Mandakova et al. 2008; Lan & Albert 2011; Sousa et al. 2014). FISH has also been successfully used to detect signatures of reticulate evolution (reviewed in Chester et al. 2010).

Amaryllidaceae tribe Hippeastreae is composed of approximately 12 genera and ca. 180 species (Meerow & Snijman 1998; Meerow et al. 2000; Meerow 2010), with a major center of diversification in Chile and western Argentina, and a second in eastern Brazil and central/northern Argentina. Although the major species richness of the tribe is in South America, *Habranthus* and *Zephyranthes* show another center of diversity in Mexico and are also found in the Greater Antilles, Florida, Texas, and the southwestern United States (Meerow & Snijman 1998). Despite the taxonomic attention that

Hippeastreae has received because of its horticultural importance, generic relationships within the tribe continue to be debated (e.g. Traub 1963; Ravenna 2003; Meerow 2010), mostly due to the lack of unequivocal diagnostic morphological characters. Chromosome numbers and karyotypes may be important for diagnosing certain lineages, although this group contains clades with dysploid variation (n = 6 - 30) usually accompanied by polyploidy and aneuploidy (Flory 1977), especially in *Habranthus* and *Zephyranthes*. This complex chromosomal evolution has not been evaluated within a phylogenetic framework.

Molecular phylogenetic analyses based on nrDNA ITS sequences (Meerow et al. 2000; Meerow 2010) have helped to elucidate relationships within the tribe and have shown that certain genera – *Rhodophiala, Habranthus,* and *Zephyranthes* – are not monophyletic. García et al. (2014) increased the taxon sampling for ITS in relation to previous studies and obtained a well-resolved tree derived from chloroplast markers (i.e., *trnL-F, ndhF,* 3'*ycf1*), with the main premise that if concerted evolution has acted upon ITS following a reticulation event (Álvarez and Wendel 2003), then comparison with a phylogeny derived from organellar genomes might detect reticulate patterns, with incongruent placements of hybridizing taxa in different gene trees (Linder & Rieseberg 2004). However, widespread cytonuclear discordance was detected, and reticulation was inferred to have affected the base of the tribe's major clade, subtribe Hippeastrinae, which includes ~90% of the tribe's species diversity. This result also supported Meerow's (2010) hypothesis of ancient reticulation (i.e., hybridization) in the Hippeastreae. In contrast, the Chilean-Argentinean endemic subtribe Traubiinae shows a tree-like pattern of evolution, consistent with an apparent lack of hybridization and allopolyploidy. Given our current phylogenetic framework for the group (Meerow 2010; García et al. 2014) and the distribution of basic chromosome numbers in the lineages involved (i.e., n = 8 or 9 in *Rhodophiala bifida*, n = 9 in core *Rhodophiala*, n = 6 in *Habranthus* and *Zephyranthes*, n = 10 in *Eithea*, n = 11 in *Hippeastrum*), we have hypothesized that the putative reticulation event(s) that preceded the radiation of Hippeastrinae most likely consisted of homoploid hybridization(s). However, allopolyploidizations are likely to have been involved in the more recent diversification of the *Habranthus-Sprekelia-Zephyranthes* complex, as suggested by polyploid series of taxa based mostly on x = 6 and cytogenetic evidence (Naranjo 1974; Flory 1977; Greizerstein and Naranjo 1987).

In this study I aim to analyze copy number variation of rDNA FISH markers and chromosome numbers to gain insights into and examine shallow allopolyploid events, especially those involving the *Habranthus-Sprekelia-Zephyranthes* complex (García et al. 2014). Ribosomal DNA 5S and 45S loci are routinely used as FISH markers for comparative analyses because of their highly conserved sequences across angiosperms, repetitive nature, and high interspecific variation in copy number and location (reviewed in Weiss-Schneeweiss and Schneeweiss 2013). Additionally, probabilistic models of chromosome number evolution will be used to infer ancestral haploid chromosome numbers of major clades (e.g., Hippeastreae, Hippeastrinae, Traubiinae) and the relative importance of various mechanisms of transitions in chromosome number (i.e., gain, loss, polyploidy, demi-polyploidy) throughout the phylogeny of Hippeastreae. I also hoped to discover putative chromosomal synapomorphies based on the current phylogenetic framework for the group (García et al. 2014; Chapter 3 of this dissertation).

Materials and Methods

Chromosome Preparations

Actively growing root tips were obtained from N. García's bulb and seed research collection, which is maintained at the UF Department of Biology Greenhouse. The apical 2 cm of growing roots were collected, usually in the morning, and treated either in an aqueous solution of 2 mM 8-hydroxyquinoline (Sigma-Aldrich, St. Louis, Missouri) for 17-20 hours at room temperature or with nitrous oxide in a sealed chamber for 2-3 hours. Over the course of almost five years of cytogenetic work, different options of collecting time and pretreatment methods were tried. In general, root tips were fixed in ice-cold 90% glacial acetic acid for 20 minutes and stored in 70% ethanol at -20ºC. Metaphase chromosome spreads were obtained by enzymatic digestion as described previously (Birchler et al. 2008).

FISH

All probes were labeled by nick translation following Birchler et al. (2008) and Chester et al. (2012). We used *Tragopogon* probes for 5S (Cy3 label) and 45S rDNA (fluorescein label) to perform FISH experiments as described in Chester et al. (2012). After hybridization, a drop of Vectashield containing DAPI (Vector Laboratories, Burlingame, California) was added to each slide before mounting a glass coverslip (Corning Incorporated, Corning, New York). Slides were stored in a black box at -4ºC.

Slides were viewed with a Zeiss Axio Imager.M2 fluorescence microscope, with fluorescence illumination provided by an X-Cite Series 120 Q Lamp (EXFO Life Sciences). Images were captured with a 100× or 63× objective lens and a microscope mounted AxioCam MRm digital camera (Zeiss) in conjunction with Axiovision version 4.8 software (Zeiss) on a PC. The Axiovision software was used to aply color to the acquired images as follows: DAPI was colored blue, the 5S rDNA probe was colored red, and the 45S rDNA probe was colored green. All images were exported at 300 pixels per inch in TIF format into Adobe Photoshop CS3 version 10.0.1 to adjust brightness and add arrows to indicate rDNA signals.

Inference of Chromosome Number Evolution

Evolutionary changes in chromosome number were inferred under a maximum likelihood (ML; Felsenstein 1973) framework using ChromEvol version 2.0 (Mayrose et al. 2010; Glick and Mayrose 2014). This software allows the evaluation of eight models of chromosome number variation with the following parameters: polyploidization (chromosome number duplication) with rate ρ, demi-polyploidization (polyploids derived from the fusion of gametes with different ploidal levels) with rate μ, and dysploidization (ascending, chromosome gain rate λ; descending, chromosome loss rate δ), as well as two linear parameters, λ_1 and δ_1, for the dysploidization rates λ and δ, to allow them to depend on current chromosome numbers. Four of the models have a constant rate, whereas the other four include the two linear parameters. Both model sets also have a null model that assumes no polyploidization events. All models were fitted to the data using an ML phylogram, in each case with 10,000 simulated repetitions to compute the expected number of changes of the four transition types along each branch of the phylogeny. The maximum number of chromosomes was set to twice the highest number found in the empirical data, and the minimum to 2.

ChromEvol inferences were performed on phylogenetic trees derived from the ITS and cpDNA data sets of García et al. (2014), to account for phylogenetic uncertainty and reticulate evolution. *Cyrtanthus* sp. (2*n* = 18) and *Worsleya procera* (2*n* = 42; Griffinieae) were removed as outgroups. Both alignments were further reduced to taxa with a known chromosome count as reported in García et al. (2014). When a species had multiple reported counts, only the lowest number was used. Both alignments were then reanalyzed under ML in RAxML ver. 8.0.25 (Stamatakis 2014). Tree searches were conducted using the rapid hill-climbing algorithm (Stamatakis 2006) with 100 independent searches starting from randomized parsimony trees with the GTRGAMMA model and four discrete rate categories; the resulting phylograms were used as ChromEvol inputs. Three analyses were performed for each data set: the first with no fixed root number (the program optimizes this value), and two subsequent analyses with different fixed root numbers, *n* = 6 and 11, respectively. Additional analyses were conducted over nuclear (9 LCNGs + ITS) and total evidence (nuclear + cpDNA) species trees for 43 diploid species (Chapter 3 of this dissertation), without fixing the root number. The best-fit model was selected based on the Akaike Information Criterion (AIC) value as reported by the ChromEvol output.

Results

rDNA FISH

FISH experiments were conducted for 21 Hippeastreae species (Table 4-1), seven from subtribe Traubiinae (Figures 4-1 and 4-2) and 14 from subtribe Hippeastrinae (Figures 4-3, 4-4, 4-5, and 4-6). FISH signals are described for 45S and 5S rDNA in Table 4-2. The only major lineage lacking FISH data is *Hippeastrum* because no suitable metaphase spreads were obtained from sampled root tips.

Within the Traubiinae, a medium-sized submetacentric chromosome carries a 45S signal most frequently in a terminal position on the short arm; however, the chromosome bearing 45S is subtelocentric in *Traubia modesta* and *Rhodolirium montanum*. *Phycella cyrtanthoides*, *Rhodolirium speciosum*, and *Famatina maulensis* have a second 45S array in a chromosome and position similar to the first array (Table 4-2). For 5S rDNA, *T. modesta*, *R. laetum*, and *R. montanum* carry an array in a large metacentric chromosome; however the position of the signal is variable (Table 4-2). The latter two species carry a second 5S rDNA array of low signal intensity that seems to be a univalent in *R. montanum* (Figure 4-1). The four species sampled from the *Phycella-Placea* clade (García et al. 2014; Chapter 3 of this dissertation) have a single 5S rDNA array on the short arm of the same chromosome that carries 45S, but in a more centromeric position (Figure 4-2).

More variation in terms of copy number and location was detected for subtribe Hippeastrinae (Table 4-2). Most diploid species have one or two 45S rDNA arrays; in contrast, most have at least two 5S rDNA arrays, except *Z. mesochloa* and *Z. flavissima*, which have a single 5S array. Trivalent signals in *Z. guatemalensis* suggest a triploid origin for this species (Fig. 4-5; Table 4-2).

Chromosome Number Evolution

Independent of the treatment, slightly different models were selected as best fit when running ChromEvol for the ITS and cpDNA trees (Tables 4-3 and 4-4). Models that include additional parameters for the chromosome gain and loss rates (making them linearly dependent on the current chromosome numbers) and a polyploidy rate parameter were chosen in all cases. However, for the ITS tree the selected model (M6) includes a demi-polyploidy rate parameter different from the polyploidy rate parameter, while for the cpDNA tree, the model (M5) only includes a polyploidy rate parameter (i.e., no demi-polyploidization events are inferred). The non-fixed root treatments had slightly lower log-likelihood and AIC scores than when the root was fixed at either $n = 6$ or $n = 11$ (Tables 4-3 and 4-4); therefore, noteworthy results (> 0.5) for the respective best fit models in the non-fixed root number treatments for ITS and cpDNA data sets are represented in Figures 4-7 and 4-8, respectively.

The ancestral haploid chromosome numbers, which we refer to here as *a* (following Chacón et al. 2014 and Sousa et al. 2014), inferred for the common ancestors of Hippeastreae and Hippeastrinae are weakly supported by the marginal likelihood reconstruction ($p < 0.5$) and were dependent on the tree used (Figures 4-7 and 4-8). According to the joint likelihood, the common ancestors of both clades are reconstructed with $a = 6$ when considering the ITS topology, while $a = 11$ is more likely given the cpDNA tree. Ancestral numbers inferred along the backbone of the trees were weakly supported based on the marginal likelihoods, except for those major clades that are consistent between trees: $a = 11$ for *Hippeastrum* (or core-*Hippeastrum* in cpDNA tree), $a = 9$ for core-*Rhodophiala/Myostemma* clade, and $a = 8$ for Traubiinae ($p > 0.5$; Figures 4-7 and 4-8). In contrast, *a* is somewhat equivocal for clades in the *Habranthus-Zephyranthes* complex (sensu García et al. 2014) and depends on the tree used. In general, $a = 6$ or 7 are inferred for clades that contain diploid *Habranthus* and *Zephyranthes*, while $a = 12$ or 24 are retrieved for the common ancestor of North American Zephyranthes lineages (see Figures 4-7 and 4-8).

In contrast, the same model was selected for analyses performed over diploid species trees (Table 4-5). The preferred model in these cases (M4) does not include additional parameters for the chromosome gain and loss rates and no duplications are inferred. Concerning the ancestral numbers for Hippeastreae and Hippeastrinae in particular, *a* = 10 is inferred for both clades over the nuclear species tree based on the joint likelihood (Fig. 4-9); however, the marginal likelihood inferred *a* = 10 and *a* = 11 as almost equally likely for Hippeastrinae (*p* = 0.48 and *p* = 0.43, respectively). When the total species tree topology is considered, *a* = 12 is inferred for Hippeastreae and *a* = 11 for Hippeastrinae (Fig. 4-10). Overall, the ancestral number for Hippeastreae is ambiguously inferred.

According to all analyses performed, more events of descending dysploidy (loss) are inferred in the chromosome number evolution of Hippeastreae than events of ascending dysploidy (gain) (Tables 4-3, 4-4, 4-5). Demi-duplications are considered only in the model selected for the ITS topology, most notably in the evolution of the *Z. albiella-puertoricensis* clade and of two terminal branches (species), *Haylockia americana* (2*n* = 18) and *Zephyranthes andina* (2*n* = 20). Two additional events of demi-duplication are weakly inferred in the branches leading to *Hippeastrum* and to *Sprekelia*.

Almost the same number of duplication events are inferred for the ITS and cpDNA trees, nine and ten for the former and latter trees, respectively, although there are some differences in the clades/species involved due to topological incongruence. Species that are consistently inferred to be polyploid in both trees include *Z. filifolia*, *Z. bifolia*, *Z. candida*, *Z. simpsonii*, *H. tubispathus*, both *Sprekelia* sp. (as two independent events in the cpDNA tree), and all Mexican/Texan *Zephyranthes* sp. with 2*n* = 48 (as three independent events in the cpDNA tree). Additional polyploid events involve the origin of *Habranthus immaculatus* based on the ITS tree and the *Z. albiella-puertoricensis* clade in the cpDNA tree. A polyploid origin for North American

Zephyranthes sp. with 2*n* = 24 (i.e., derived from 2*n* = 12) is not implied in the cpDNA tree; however, based on the ITS analysis a putative polyploid event gave rise to *Z. carinata* at the base of the Mexican/Texas clade, and a demi-duplication derived from 2*n* = 18 is inferred for the main clade that contains *Z. rosea* (Cuba), *Z. atamasco*, and *Z. treatiae* (southeastern U.S.).

Discussion

rDNA FISH

Extensive variation in numbers and chromosomal locations of rDNA loci among closely related species has been observed in several plant groups (reviewed by Weiss-Schneeweiss and Schneeweiss 2013), including other monocots such as *Alstroemeria* (Alstroemeriaceae; Chacón et al. 2012), *Paphiopedilum* (Orchidaceae; Lan and Albert 2011), *Iris* subgenus *Xiphium* (Iridaceae; Martinez et al. 2010), *Typhonium* (Araceae; Sousa et al. 2014), and *Eleocharis* (Cyperaceae; Da Silva et al. 2010). Similar results in terms of species/lineage-specific rDNA configurations have been found in groups more closely related to Hippeastreae, such as *Lycoris* (Amaryllidaceae; Chang et al. 2009) and *Allium* (Alliaceae; Lee et al. 1999). The instability of rDNA sites has been related to their transcriptional ability (Butler 1992); 45S in particular has been reported as a preferred site for chromosome rearrangements and chromosome breakage-fusion-bridge cycles in telomerase-deficient *Arabidopsis* (Siroky et al. 2003) and has been described as a fragile site in plant genomes (Huang et al. 2012).

Although fewer studies have been conducted above the species level, they all highlight widespread variation in number and location of rDNA loci that can eventually constitute synapomorphies for certain evolutionary lineages (e.g., Brassicaceae, Hasterok et al. 2006; Asteraceae, Garcia et al. 2010; Abd El-Twab and Kondo 2012; the phaseoloid clade of Fabaceae, reviewed in Iwata et al. 2013; Ranunculaceae tribe Anemoninae, Mlinarec et al. 2011). The results of FISH experiments in Hippeastreae show that nearly every analyzed species is characterized by a unique rDNA constellation, and given our current knowledge of Hippeastreae phylogeny, a few putative synapomorphies were identified and are discussed in the following paragraphs.

The co-localization of 45S and 5S loci on the short arm of a medium submetacentric chromosome is a putative synapomorphy of the *Phycella-Placea* clade. This chromosome was also found in *Placea amoena* Phil. (Baeza and Schrader 2004); however, this species shows greater variation in 5S, with four arrays present, at least twice the number found in the members of the *Phycella-Placea* clade studied here. Among these, *Placea arzae* shows only one 5S array (the one co-localized with 45S), while the remaining three have an additional 5S array. Co-localized 5S-45S loci are usually considered rare among angiosperms; however, they have also been reported from other monocots such as *Lilium* (Lim et al. 2001), *Alstroemeria* (Chacón et al. 2012), *Maxillaria* (Cabral et al. 2006), *Iris* (Martínez et al. 2010), and *Lycoris* (Chang et al. 2009). Copy-number variation in rDNA loci between closely related species at the diploid level, such as that found between Traubiinae taxa, has been explained by several mechanisms that can act alone or in combination, such as chromosomal rearrangements, dynamic double-strand break repair processes in pericentromeric and telomeric regions, homologous and non-homologous crossing-over, and the action of transposable elements (Schubert and Wobus 1985; Schubert and Lysák 2011).

The rDNA configuration found for both core-*Rhodophiala* members studied here (i.e., *R. advena*, *R. araucana*) is a putative cytogenetic synapomorphy for that clade.

The same configuration, i.e., one 45S array terminal in the long arm of a submetacentric and two 5S arrays terminal in the long arms of a submetacentric and a subtelocentric chromosome, respectively, was also reported for *Rhodophiala* aff. *advena* by Baeza et al. (2006). The sample analyzed by these authors comes from a distant location to the *R. advena* analyzed here, and it is very probable that it corresponds to *Rhodophiala splendens* Renjifo or *R. maculata* (L'Hér.) Ravenna. However, it is uncertain whether this putative synapomorphy characterizes the entire core-Rhodophiala clade because data for *Famatina herbertiana* (Lindl.) Ravenna are lacking. This species has been consistently inferred as part of the core-*Rhodophiala* clade and sister to all Chilean-Argentinean members of that group (Meerow 2010; García et al. 2014; Chapter 3 of this dissertation); however, there is not even a chromosome count available for this taxon. The same issue arises with regard to the ancestral haploid number of 9 inferred for this clade: does it apply to the entire clade, or to all species except *F. herbertiana*?

Copy number of rDNA loci does not seem to follow a strict linear pattern relative to chromosome number or putative ploidy (see Tables 4-2 and 4-3). The highest number of 45S signals is found in *Z*. aff. *bakeriana* (2*n* = 30 + 1B) with four arrays; however, two species with slightly higher chromosome numbers, *Z. albiella* (2*n* = 32) and *Z. guatemalensis* (2*n* = 36), show three 45S arrays each, and only two were detected in the species with the highest chromosome numbers, *Z. citrina* (2*n* = 48) and *S. howardii* (2*n* = 60). Despite being clearly diploid, *Habranthus robustus* (2*n* = 12) has the highest number of 5S signals, with six arrays. The non-linear relationship between chromosome number, ploidy, and copy number of rDNA loci is considered a general evolutionary trend in angiosperms (Weiss-Schneeweiss and Schneeweiss 2013). The rates and mechanism of variation seem to differ between 5S and 45S loci within a genome, and might be group-specific (Weiss-Schneeweiss and Schneeweiss 2013). 45S rDNA loci are in general more prone to undergo rapid homogenization, silencing, and loss of loci, especially in polyploids (e.g., Kovařík et al. 2005; Weiss-Schneeweiss et al. 2008; Kotseruba et al. 2010). Both types of rDNA loci are differentially affected by genome diploidization in polyploids and this usually involves a gradual reduction in loci number, which roughly correlates with the polyploid's age (Clarkson et al. 2005).

A denser taxon sampling for FISH experiments would have been preferable, especially within Hippeastrinae, which is the most challenging clade in terms of the inference of phylogenetic relationships (García et al. 2014). For instance, the inclusion of additional diploid *Zephyranthes* and *Habranthus* sp. might have resulted in more insightful inferences of the mechanisms of chromosomal evolution in this group. The lack of *Hippeastrum* in the current sampling is also a hindrance, considering that this genus constitutes one of the major lineages of Hippeastrinae. The karyotypes of *Hippeastrum* have been studied extensively elsewhere (Naranjo and Andrada 1975; Arroyo 1982; Naranjo and Poggio 1998; Brandham and Bhandol 1996), and the 5S location in a tetraploid cytotype of *H. reticulatum* ($2n = 44$) has been reported (Brogliato 2014). The latter study and the present one include *Tocantinia* sp., a species that has the same chromosome number as most *Hippeastrum* ($2n = 22$) and is sister to a *Hippeastrum* s. s. clade in species tree analyses (Chapter 3 of this dissertation). More FISH markers also seem necessary to trace chromosome rearrangements across the evolutionary scale studied here, especially considering that the phylogeny of Hippeastreae is likely to be reticulate at the diploid and polyploid levels. Despite sparse taxon sampling and few markers, some insights were gained, and this study should be considered as a first step towards understanding karyotype evolution of the Hippeastreae.

Chromosome Number Evolution

Our current knowledge of Hippeastreae phylogeny (Meerow 2010; García et al. 2014; Chapters 2 and 3 of this dissertation) suggests that a bifurcating tree might not be the best model to represent the evolutionary history of this group. Current ancestral reconstruction methods work only over bifurcating trees, and no methods have yet been developed to infer ancestral states over phylogenetic networks. Even though I attempted to account for reticulate evolution by running the model over two disparate trees, such as those retrieved by ITS and cpDNA sequence data, the results of these analyses must be interpreted with caution.

Interpreting patterns of gains and losses of chromosomes is difficult, especially when both are inferred over the same branch. Overall, evolution by descending dysploidy and polyploidy seem to be the most relevant mechanisms of chromosome evolution in Hippeastreae based on analyses using ChromEvol; however, this method does not inform about potential occurrences of diploid and homoploid hybridizations, which could have consequences for chromosome number evolution. Diploid hybridization has been implicated in the origin of Hippeastrinae (García et al. 2014), and more recent analyses based on low-copy nuclear genes (Chapter 3 of this dissertation) suggest that these hybridization events were more likely restricted to the generation of $2n = 18$ lineages, i.e., *Rhodophiala bifida*, *Eithea*, and core-*Rhodophiala,* each of which seems to have had an independent origin.

Concerning other chromosome numbers in Hippeastrinae, 2*n* = 22 has been postulated as the most likely ancestral number for Amaryllidaceae given its ubiquity throughout the family (Flory 1977; Meerow 1984, 1987; Meerow and Snijman 1998). Furthermore, two of the four analyses of chromosome number evolution performed here infer *a* = 11 as the most likely ancestral number for Hippeastrinae. Given the inference of more losses than gains in these modeling analyses, it also seems reasonable to argue that most other diploid chromosome numbers are derived from 2*n* = 22 within Hippeastrinae. Besides its occurrence in *Hippeastrum* and *Tocantinia* sp. within the Hippeastreae, 2*n* = 22 is found in at least one genus of most African and Eurasian tribes (Meerow and Snijman 1998). Within the American clade, it has been postulated that an ancestral stock of 2*n* = 22 was involved in the origin of the Andean tetraploid clade (tribes Eustephieae, Hymenocallideae, Clinantheae, and Eucharideae) that is characterized by a most common somatic chromosome number of 2*n* = 46 (Meerow 1984, 1987; Meerow and Snijman 1998). The latter number could have arisen from 2*n* = 22 through chromosome fragmentation or duplication and subsequent doubling (Satô 1938, Lakshmi 1978), or by deep reticulation between ancestral 2*n* = 22 and 2*n* = 24, followed by doubling (Meerow and Snijman 1998).

Other diploid chromosome numbers that are frequent in Hippeastreae seem recursive within Amaryllidaceae and most have been interpreted as derivatives of 2*n* = 22 (Meerow and Snijman 1998). For instance, 2*n* = 16 is likely a synapomorphy for Traubiinae and is also a prevalent number in African *Cyrtanthus* (Cyrtantheae), *Scadoxus*, and *Hemanthus* (Haemantheae) (Meerow and Snijman 1998). Through a detailed comparative analysis of karyotypes, Ising (1966, 1968, 1969, 1970) inferred widespread structural rearrangements while mostly preserving the same chromosome number in *Cyrtanthus*.

On the other hand, $2n = 12$ is found elsewhere within Amaryllidaceae in Eurasian *Lycoris* (Lycoridae) and African *Apodolirion* and *Gethyllis* (Haemantheae); the latter genera show interesting convergence with certain Hippeastreae by having a single-flowered scape with fused spathe valves (as in *Habranthus* and *Zephyranthes*) and a suppressed scape elongation (as in *Haylockia*) (Meerow and Snijman 1998). A complement $2n = 14$ is, however, more ubiquitous than the latter and can be found in certain African and Eurasian genera that also have species with $2n = 22$, including *Cyrtanthus*, *Lycoris*, *Narcissus* (Narcisseae), and *Leucojum* (Galantheae) (Meerow and Snijman 1998). Besides the two numbers just mentioned, $2n = 18$ can be also be found in the Eurasian genera *Lycoris* and *Leucojum*. Therefore, a better understanding of chromosome number trasitions in other Amaryllidaceae groups could provide some hints about karyotypic evolution in the Hippeastreae.

The ChromEvol model introduced the controversial concept of demi-duplications (Mayrose et al 2010; Mayrose and Brick 2014) to reflect, for instance, the cross of a reduced gamete and another gamete with twice its number (unreduced gamete or reduced gamete of a tetraploid). This concept implies a triploid bridge in chromosome number evolution and is supported by examples mentioned by Ramsey and Schemske (1998). In the context of the origin of $2n = 18$ karyotypes in Hippeastreae, this mechanisms seem possible based on $a = 6$ ($n = 6 + n = 12 \rightarrow 2n = 18$). Flory and Flagg (1958) reported that reciprocal crosses between *Habranthus robustus* ($2n = 12$) and *H. brachyandrus* ($2n = 24$) generate hybrids with 18 somatic chromosomes that occur in three groups of six metacentrics, submetacentrics, and subtelomerics, respectively. This hybrid is mostly sterile, but one out of six flowers produces a capsule with four to five viable seeds if self-pollinated (the parental species produce capsules with 50-60 viable seeds), which is interpreted as a potentially common process in nature related to speciation following hybridization in this group (Flory and Flagg 1958). Referring to the ChromEvol analyses, the only 2*n* = 18 taxon that was inferred as a product of demi-duplication is *Haylockia americana*, a clear member of the *Habranthus-Zephyranthes* complex, which is largely a series of multiples of 6. The only image of a chromosome spread for *Haylockia americana* was reported by Flory (1977), and it does not show evident signs of triploidy; however, there are no data on meiotic behavior, and diploidization might have acted over time since the origin of this species. *Haylockia americana* is certainly an interesting candidate to explore with FISH experiments.

Alternatively, 2*n* = 18 could have arisen by the loss of two chromosome pairs, by the fusion of four chromosome pairs, or a combination of both mechanisms from a 2*n* = 22 ancestor. This hypothesis was proposed by Naranjo and Poggio (2000) to explain the origin of *Rhodophiala bifida* and to suggest that the 2*n* = 16 cytotype was derived from 2*n* = 18 by a process of chromosome reduction that involved reciprocal translocations. The present study only included the 2*n* = 16 cytotype of *R. bifida*; more work on this species (or complex of species) is necessary, including both cytotypes and sampling throughout its distribution.

A third option proposed here is the cross of 2*n* = 22 and 2*n* = 14 (*n* = 11 + *n* = 7 ➔ 2*n* = 18). This pathway seems plausible based on a) the putative hybrid origin of 2*n* = 18 lineages based on phylogenetic analyses (Chapter 3 of this dissertation), b) the cross implies two reduced gametes which seems more likely and parsimonious than other options, c) $2n = 22$ is the typical number in *Hippeastrum* (Naranjo and Andrada 1975; Naranjo and Poggio 1988), and $2n = 14$ is found in certain diploid *Habranthus* and *Zephyranthes* (Naranjo 1974; Greizerstein and Naranjo 1987), and d) ChromEvol inferred $a = 7$ as a likely ancestral haploid chromosome number for certain *Habranthus-Zephyranthes* clades in all trees considered, despite the fact that $n = 7$ is not well represented in the sampled taxa. To illustrate the last point, $a = 7$ is inferred for the most inclusive clades that contains *Habranthus pedunculosus* Herb. ($2n = 12, 14$; Flory and Flagg 1958; Naranjo 1974; S. Arroyo-Leuenberger, pers. comm.) in ITS, cpDNA, and total trees. Yet, the most commonly reported number for this taxon is $n = 7$ (Flory and Flagg 1958 as *H. juncifolius* Traub & Hayward; Naranjo 1974 as *H. teretifolius* (C. H. Wright) Traub & Moldenke). A single or most likely mechanism for the origin of $2n = 18$ lineages is not implicit with the available data. The origin of these clades, specifically whether they involved hybridizations or only aneuploidy/dysploidy, is of great significance for understanding the evolutionary pattern in Hippeastrinae.

The origin of diploid Hippeastreae lineages does not seem to have involved cryptic whole-genome duplications according to ChromEvol analyses. However, polyploidy is very prevalent in the diversification of the *Habranthus-Zephyranthes-Sprekelia* complex, and the reticulate pattern of evolution in this group further complicates the inference of these events, as in the case of $2n = 24$ *Zephyranthes* spp. This chromosome number can be also found in African *Cryptostephanus* (Haemantheae) and Eurasian *Galanthus* (Galantheae). In neither case is the origin of $2n = 24$ clear; however, within Hippeastreae this number has been traditionally interpreted as derived through allopolyploidy from 2*n* = 12 (e.g., Flory 1977, Greizerstein and Naranjo 1987). Studies conducted in *Z. rosea* Lindl. (Tandom and Mathur 1965) and in *Z. tubispatha* Herb. (Lakshmi 1980) have reported 12 bivalent pairs at meiosis for these 2*n* = 24 species, which suggests that these might have been derived by an ancient allopolyploid event due to the diploidization of the karyotype.

Synthesis and Future Directions

The *Placea-Phycella* and core *Rhodophiala* clades seem to be the most distinct cytogenetic lineages of Hippeastreae – each have putative synapomorphic rDNA configurations and chromosome numbers. No evident link can be made in terms of cytology beween the core-*Rhodophiala* clade and the *Habranthus-Zephyranthes* complex, mainly due to sparce taxon sampling and high variation in the latter group.

It seems that 2*n* = 22, 18, and 12 are equally likely as ancestral chromosome numbers for Hippeastreae and subtribe Hippeastrinae based on the probabilistic model of chromosome number evolution. However, if the ancestral number for Amaryllidaceae s. s. is 2*n* = 22 (Flory 1977; Meerow 1984, 1987; Meerow and Snijman 1998; Naranjo and Poggio 2000) and taking into account the relevance of fission/loss inferred by probabilistic models, *Hippeastrum* could be hypothesized as a direct descendant of the ancestral Hippeastreae lineage (and probably of all American Amaryllidaceae, considering that nowhere outside of this clade (including *Tocantinia* sp.) does this number occur within American amaryllids). Major diploid offshoots from the ancestral 2*n* = 22 stock might have resulted through descending dysploidy (chromosome fusions) or aneuploidy (chromosome/DNA loss) or a combination of both mechanisms.

In this way, *Griffinia* (2*n* = 20; Meerow et al. 2002) could have emerged by the loss of one chromosome pair or alternatively by the fusion of two chromosome pairs.

Similarly, the origin of subtribe Traubiinae ($2n = 16$) might have involved the loss of three chromosome pairs or a combination of chromosome/DNA loss and chromosome fusions (this seems more likely than considering the fusion of three chromosome pairs as a sole mechanism). The transition between $2n = 22$ to $2n = 12$ within the Hippeastrinae clade most likely involved both mechanisms (dysploidy and aneuploidy) as well. The mechanisms involved in the origin of the $2n = 18$ lineages are not yet clear, although hybridization was potentially involved. A detailed comparative analysis of karyotype morphology is needed to test these hypotheses, but is beyond the scope of the current study.

An Amaryllidaceae-wide analysis of chromosome number evolution might improve the inference of ancestral haploid chromosome numbers for major clades, including evaluation of the hypothesis that $n = 11$ is the ancestral number of Amaryllidaceae s. s. and resolving the ancestral numbers for Hippeastreae and Hippeastrinae. Future studies should increase the sampling of Hippeastrinae, focusing on diploid taxa and including additional FISH markers to provide further insights into the early evolution of this clade, mechanisms involved in shifts of basic chromosome numbers, and putative ancient hybridizations. Finally, additional comparative data on genome sizes would be desirable to discern mechanisms of chromosome loss/gain among the main diploid lineages.

Table 4-1. Samples and spread numbers for FISH experiments.

Species	Voucher
Subtribe Traubiinae	
Famatina maulensis	N. García 4384 (CONC, FLAS)
Phycella cyrtanthoides	N. García 4386 (FLAS)
Placea arzae	N. García 3025 (CONC)
Rhodolirium laetum	M. Rosas 4230 (CONC)
Rhodolirium montanum	N. García 4379 (FLAS)
Rhodolirium speciosum	I. Lizama s.n. (CONC)
Traubia modesta	O. Fernández 151 (JBN-Chile)
Subtribe Hippeastrinae	
Eithea blumenavia	J. Dutilh s.n. (UEC)
Habranthus robustus	N. García 4390 (FLAS)
Rhodophiala advena	N. García 2964 (CONC, FLAS)
Rhodophiala araucana	N. García 4345 (CONC, FLAS)
Rhodophiala bifida	A. Meerow 3102 (FTG)
Sprekelia howardii	D. Lehmiller 1940 (TAMU)
Tocantinia sp.	N. García 4400 (FLAS)
Zephyranthes aff. *bakeriana*	B. E. Leuenberger 3971 (B)
Zephyranthes albiella	N. García 4375 (FLAS)
Zephyranthes citrina	N. García 4376 (FLAS)
Zephyranthes flavissima	N. García 4388 (FLAS)
Zephyranthes guatemalensis	N. García 4392 (FLAS)
Zephyranthes mesochloa	B. E. Leuenberger 4494 (B)
Zephyranthes rosea	N. García 4377 (FLAS)

Table 4-2. Description of 45S and 5S rDNA patterns in FISH experiments.

		Number of rDNA sites					Positions of rDNA sites	
		45S		5S		45S + 5S		
Taxon	2n	major	visible sites	major	visible sites	Co-localization	45S	5S
Traubiinae								
Traubia modesta	16	2	2	2	2	0	t	st
Rhodolirium laetum	16	2	2	2	4	0	t	t, i
Rhodolirium montanum	16	2	2	2	3	0	t	t, i
Placea arzae	16	2	2	2	2	2	t	st
Phycella cyrtanthoides	16	4	4	2	2	2	t	st
Famatina maulensis	16	4	4	2	2	2	t	st
Rhodolirium speciosum	16	4	4	2	2	2	t	st
Hippeastrinae								
Rhodophiala bifida	16	2	2	2	4	0	t	t, c
Rhodophiala advena	18	2	2	2	4	0	t	t
Rhodophiala araucana	18	2	2	2	4	0	t	t
Eithea blumenavia	18	4	4	2	4	2	t	t, p
Tocantinia sp.	22	2	2	2	6	0	t	t, st, p
Habranthus robustus	12	2	4	2	12	2	t	t, st, i, p, c
Zephyranthes mesochloa	12	2	2	2	2	0	t	t
Zephyranthes flavissima	14	4	4	2	2	0	t	st
Zephyranthes rosea	24	4	4	2	5	0	t	t, st, p
Zephyranthes aff. *bakeriana*	30 + 1B	4	8	2	5	1	t	t, i
Zephyranthes albiella	32	4	6	4	10	0	t	t, p
Zephyranthes guatemalensis	36	3	6	3	6	3	t, st	t, st
Zephyranthes citrina	48	3	3	4	8	0	t	t, st
Sprekelia howardii	60	2	4	2	9	0	t	t, st, p, c

Table 4-3. Scores and predicted number of events for each chromosome number transition as inferred for the nrDNA ITS tree under different models. An asterisk (*) denotes the preferred model.

		Scores		Number of events			
Treatment	Model	Log-likelihood	AIC	Ascending Dysploidy (j=i+1)	Descending Dysploidy (j=i-1)	Whole-Genome Duplications (j=2i)	Demi-Duplications (j=1.5i)
Non-fixed root chromosome number	M1: Const_Rate	-162.8	331.6	85.0266	65.625	14.8767	0
	M2: Const_Rate_Demi	-159.4	324.8	37.3396	10.1317	9.74171	9.27158
	M3: Const_Rate_Demi_Est	-159.4	326.9	37.3959	10.184	11.277	10.0562
	M4: Const_Rate_No_Dupl	-211	426.1	1175.47	1103.42	52.6083	0
	M5: Linear_Rate	-156.9	323.9	31.8712	106.494	17.3323	0
	M6: Linear_Rate_Demi*	-154	317.9	24.6003	50.424	10.0967	10.6072
	M7: Linear_Rate_Demi_Est	-153.9	319.9	24.3789	45.2778	10.2416	10.3934
	M8: Linear_Rate_No_Dupl	-200.6	409.1	1105.93	1054.96	18.6421	0
Fixed root chomosome number (n=6)	M1: Const_Rate	-163	331.9	73.3635	71.7029	13.2947	0
	M2: Const_Rate_Demi	-159.8	325.6	33.0104	39.3135	8.77609	10.2697
	M3: Const_Rate_Demi_Est	-159.8	327.6	29.6086	35.9664	8.23157	11.3087
	M4: Const_Rate_No_Dupl	-216.1	436.1	885.531	850.93	38.637	0
	M5: Linear_Rate	-157.1	324.1	34.7974	86.1509	18.3225	0
	M6: Linear_Rate_Demi	-154	318.1	19.7933	49.8986	10.3762	12.0085
	M7: Linear_Rate_Demi_Est	-153.9	319.9	22.0758	47.2085	10.6733	10.206
	M8: Linear_Rate_No_Dupl	-199.4	406.8	1227.9	1183.59	19.2501	0
Fixed root chomosome number (n=11)	M1: Const_Rate	-163.8	333.7	61.0194	88.0744	11.1317	0
	M2: Const_Rate_Demi	-161.1	328.2	34.3694	68.9318	6.98836	8.09311
	M3: Const_Rate_Demi_Est	-161.1	330.2	31.2754	70.803	6.85993	8.77392
	M4: Const_Rate_No_Dupl	-211.7	427.4	1105.07	1092.57	41.854	0

Table 4-3. Continued.

Treatment	Model	Scores: Log-likelihood	Scores: AIC	Number of events: Ascending Dysploidy (j=i+1)	Descending Dysploidy (j=i-1)	Whole-Genome Duplications (j=2i)	Demi-Duplications (j=1.5i)
	M5: Linear_Rate	-157.3	324.5	34.7649	127.191	17.9915	0
	M6: Linear_Rate_Demi	-155	320	26.677	79.7267	8.29857	9.67332
	M7: Linear_Rate_Demi_Est	-155	322	26.8894	81.4318	8.13022	9.56684
	M8: Linear_Rate_No_Dupl	-199	406	1384.92	1368.47	21.1507	0

Table 4-4. Scores and predicted number of events for each chromosome number transition as inferred for the chloroplast (cpDNA) tree under different models. An asterisk (*) denotes the preferred model.

		Scores		Number of events			
Treatment	Model	Log-likelihood	AIC	Ascending Dysploidy (j=i+1)	Descending Dysploidy (j=i-1)	Whole-Genome Duplications (j=2i)	Demi-Duplications (j=1.5i)
Non-fixed root number	M1: Const_Rate	-166.2	338.4	63.5936	82.5837	16.4292	0
	M2: Const_Rate_Demi	-167.5	341	39.5657	65.3013	11.014	7.55053
	M3: Const_Rate_Demi_Est	-165.7	339.4	48.4949	65.7925	14.6239	2.59739
	M4: Const_Rate_No_Dupl	-231.6	467.3	1198.06	1124.26	49.1224	0
	M5: Linear_Rate*	-159.8	329.7	50.0877	90.8565	17.7416	0
	M6: Linear_Rate_Demi	-162.1	334.2	31.1667	98.2916	12.2682	8.06142
	M7: Linear_Rate_Demi_Est	-159.8	331.6	43.4281	90.0388	16.1787	0.92595
	M8: Linear_Rate_No_Dupl	-223.9	455.9	1284.89	1233.39	17.0831	0
Fixed root chomosome number (n=6)	M1: Const_Rate	-166.3	338.6	69.1707	81.1097	16.4778	0
	M2: Const_Rate_Demi	-167.6	341.3	47.5813	62.3206	12.7326	7.22194
	M3: Const_Rate_Demi_Est	-165.9	339.8	55.7554	66.7523	14.7951	2.50792
	M4: Const_Rate_No_Dupl	-237.5	478.9	835.257	771.472	26.7848	0
	M5: Linear_Rate	-160.2	330.4	52.2402	85.6561	17.8063	0
	M6: Linear_Rate_Demi	-162.6	335.1	31.3796	87.4188	14.242	9.65058
	M7: Linear_Rate_Demi_Est	-160.2	332.4	47.4039	85.3363	16.6765	0.63696
	M8: Linear_Rate_No_Dupl	-226	460	1030.03	949.759	20.069	0
Fixed root chomosome number (n=11)	M1: Const_Rate	-166.5	338.9	56.7411	84.4654	11.2858	0
	M2: Const_Rate_Demi	-168.1	342.2	36.1002	81.668	9.11209	5.68012
	M3: Const_Rate_Demi_Est	-166.1	340.2	50.1122	82.033	11.4227	1.74956
	M4: Const_Rate_No_Dupl	-234.1	472.2	1087.39	1007.63	36.0874	0

Table 4-4. Continued.

Treatment	Model	Scores		Number of events			
		Log-likelihood	AIC	Ascending Dysploidy (j=i+1)	Descending Dysploidy (j=i-1)	Whole-Genome Duplications (j=2i)	Demi-Duplications (j=1.5i)
	M5: Linear_Rate	-160.5	331.1	45.1388	115.044	13.9916	0
	M6: Linear_Rate_Demi	-162.5	335	25.1232	113.27	12.0505	7.99528
	M7: Linear_Rate_Demi_Est	-160.5	333	39.3023	117.784	14.9952	1.01795
	M8: Linear_Rate_No_Dupl	-225.1	458.3	1170.36	1130.32	14.7399	0

Table 4-5. Scores and predicted number of events for each chromosome number transition as inferred for diploid species trees with non-fixed root number. An asterisk (*) denotes the preferred model.

		Scores		Number of events			
Tree	Model	Log-likelihood	AIC	Ascending Dysploidy (j=i+1)	Descending Dysploidy (j=i-1)	Whole-Genome Duplications (j=2i)	Demi-Duplications (j=1.5i)
Nuclear tree (LCNGs + ITS)	M1: Const_Rate	-48.63	103.3	7.83269	27.4915	5.023e-13	0
	M2: Const_Rate_Demi	-48.72	103.4	0	37.2154	0	0
	M3: Const_Rate_Demi_Est	-47.54	103.1	14.8809	0	1.226e-10	9.02586
	M4: Const_Rate_No_Dupl*	-48.63	101.3	7.75976	27.8301	5.630e-18	0
	M5: Linear_Rate	-48.46	106.9	7.87695	26.8376	0	0
	M6: Linear_Rate_Demi	-48.46	106.9	7.79657	26.7586	0	0
	M7: Linear_Rate_Demi_Est	-48.37	108.7	15.279	0	1.713e-17	8.90966
	M8: Linear_Rate_No_Dupl	-48.46	104.9	7.9176	26.8776	0	0
Total tree (nuclear + cpDNA)	M1: Const_Rate	-50.19	106.4	0	40.7425	0	0
	M2: Const_Rate_Demi	-50.19	106.4	0	41.1272	0	0
	M3: Const_Rate_Demi_Est	-50.03	108.1	18.0094	0	4.817e-09	9.06594
	M4: Const_Rate_No_Dupl*	-50.2	104.4	0	41.2351	0	0
	M5: Linear_Rate	-50.23	110.5	9.66543	30.0458	0	0
	M6: Linear_Rate_Demi	-50.23	110.5	9.57471	29.9666	0	0
	M7: Linear_Rate_Demi_Est	-50.78	113.6	17.7438	0	6.838e-14	8.96379
	M8: Linear_Rate_No_Dupl	-50.23	108.5	9.51407	29.9058	0	0

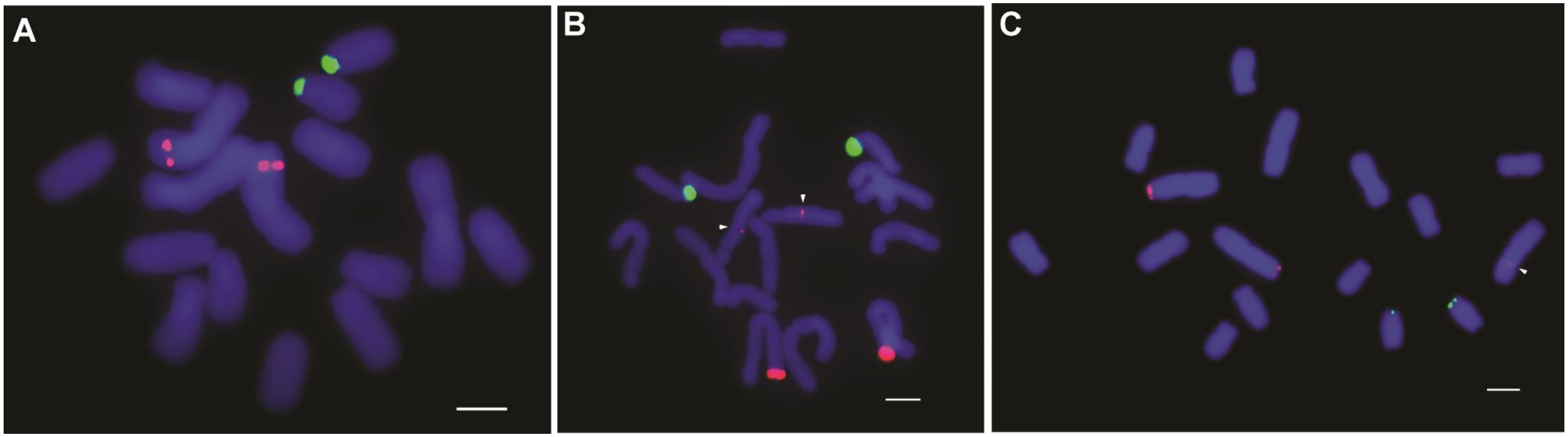

Figure 4-1. Fluorescence in situ hybridization (FISH) on mitotic metaphase chromosomes of (A) *Traubia modesta* (2*n* = 16), (B) *Rhodolirium laetum* (2*n* = 16), and (C) *Rhodolirium montanum* (2*n* = 16). Merged images of 5S rDNA (red) and 45S rDNA sites (green) over DAPI stained (blue) chromosomes. White arrowheads indicate weak 5S signals. Scale bars = 5 μm.

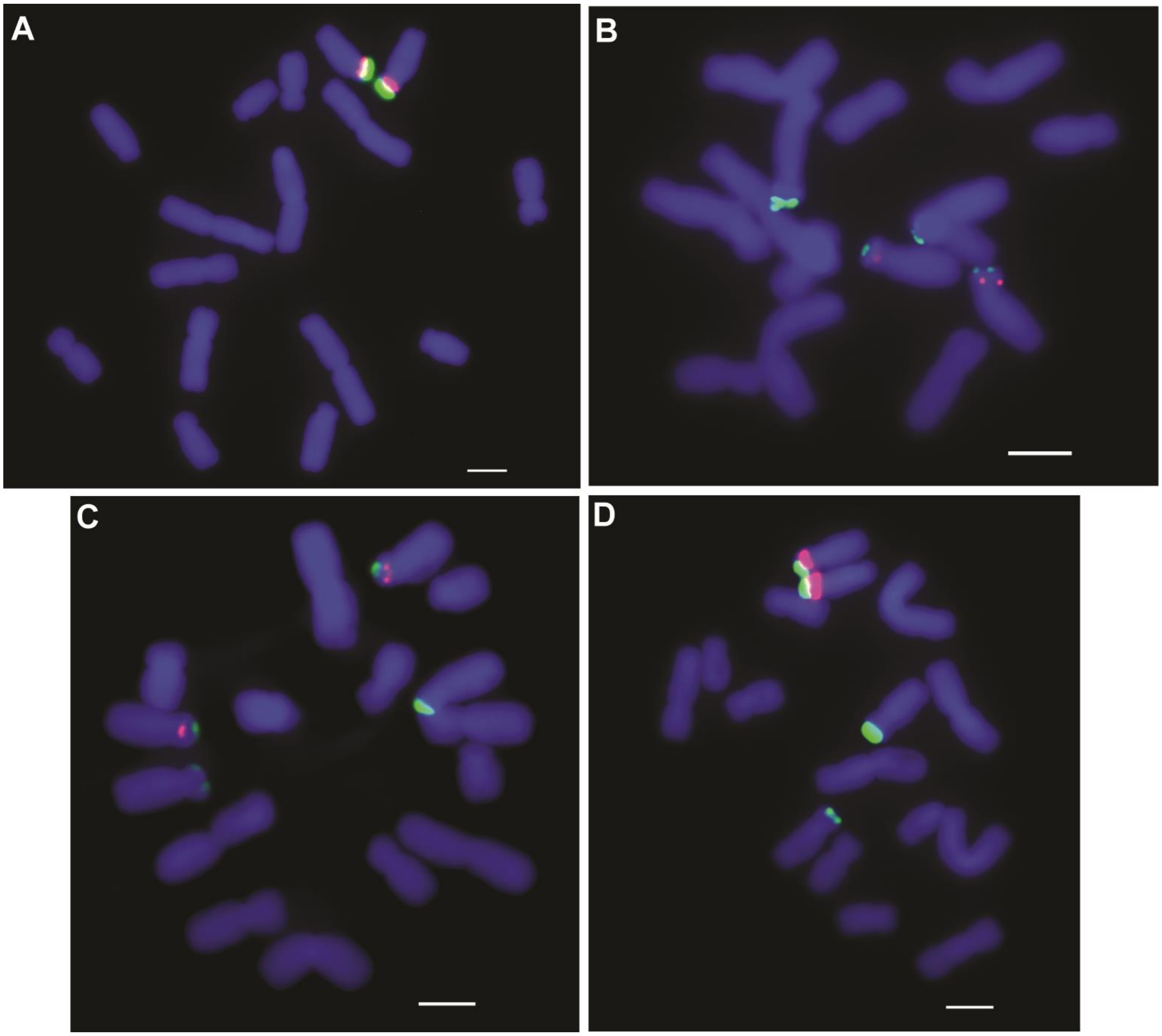

Figure 4-2. Fluorescence in situ hybridization (FISH) on mitotic metaphase chromosomes of (A) *Placea arzae* (2*n* = 16), (B) *Rhodolirium speciosum* (2*n* = 16), (C) *Famatina maulensis* (2*n* = 16), and (D) *Phycella cyrtanthoides* (2*n* = 16). Merged images of 5S rDNA (red) and 45S rDNA sites (green) over DAPI stained (blue) chromosomes. Scale bars = 5 μm.

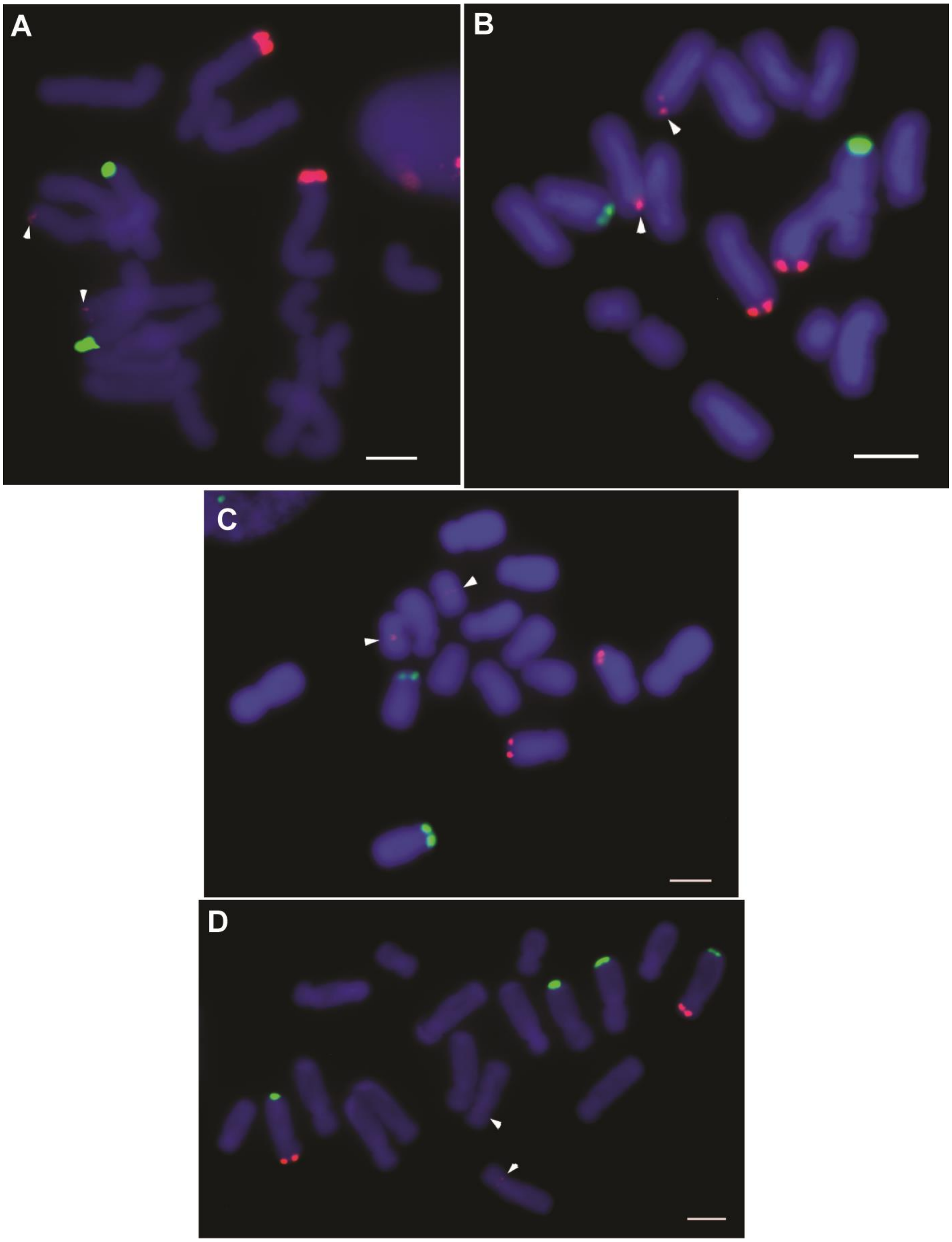

Figure 4-3. Fluorescence in situ hybridization (FISH) on mitotic metaphase chromosomes of (A) *Rhodophiala advena* (2*n* = 18), (B) *Rhodophiala araucana* (2*n* = 18), (C) *Rhodophiala bifida* (2*n* = 16), and (D) *Eithea blumenavia* (2*n* = 18). Merged images of 5S rDNA (red) and 45S rDNA signals (green) over DAPI stained (blue) chromosomes. White arrowheads indicate weak 5S signals. Scale bars = 5 µm.

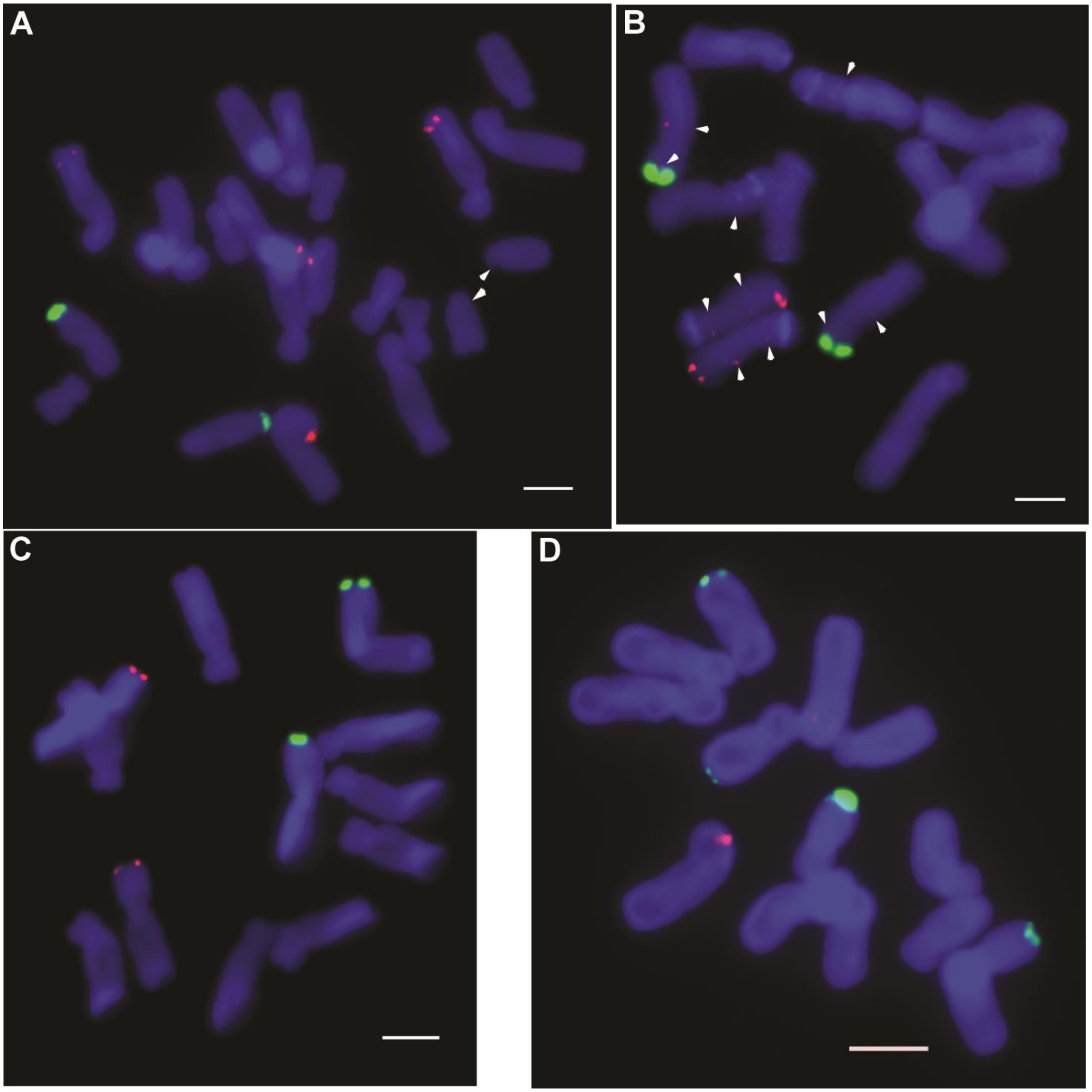

Figure 4-4. Fluorescence in situ hybridization (FISH) on mitotic metaphase chromosomes of (A) *Tocantinia* sp. (2*n* = 22), (B) *Habranthus robustus* (2*n* = 12), (C) *Zephyranthes mesochloa* (2*n* = 12), and (D) *Zephyranthes flavissima* (2*n* = 14). Merged images of 5S rDNA (red) and 45S rDNA signals (green) over DAPI stained (blue) chromosomes. White arrowheads indicate weak 5S signals. Scale bars = 5 µm.

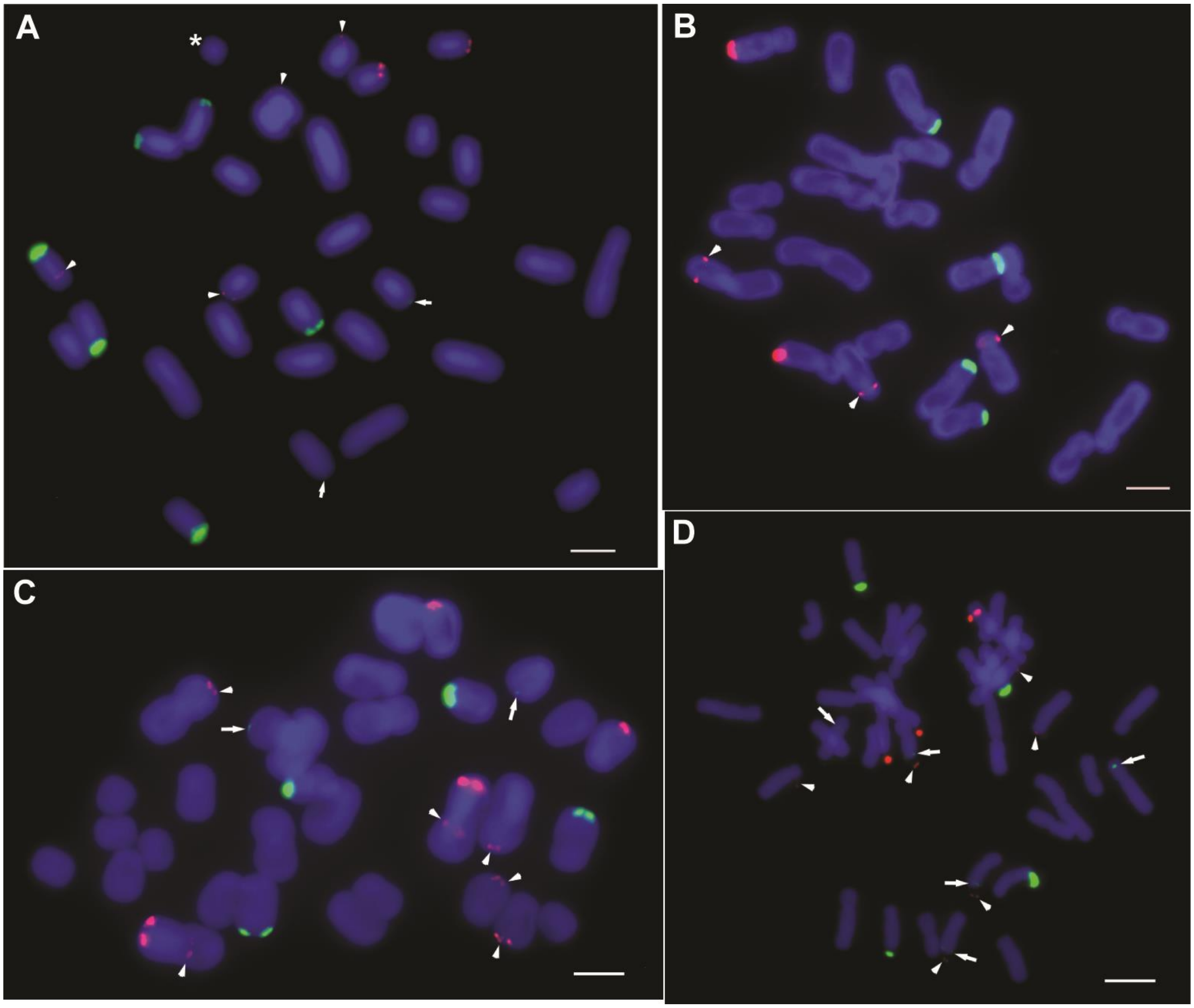

Figure 4-5. Fluorescence in situ hybridization (FISH) on mitotic metaphase chromosomes of (A) *Zephyranthes* aff. *bakeriana* ($2n$ = 30 + 1B), (B) *Zephyranthes rosea* ($2n$ = 24), (C) *Zephyranthes albiella* ($2n$ = 32), and (D) *Zephyranthes guatemalensis* ($2n$ = 36). Merged images of 5S rDNA (red) and 45S rDNA signals (green) over DAPI stained (blue) chromosomes. White arrowheads indicate weak 5S signals and white arrows denote weak 45S signal. An asterisk in (A) indicates a putative B-chromosome. Scale bars = 5 µm.

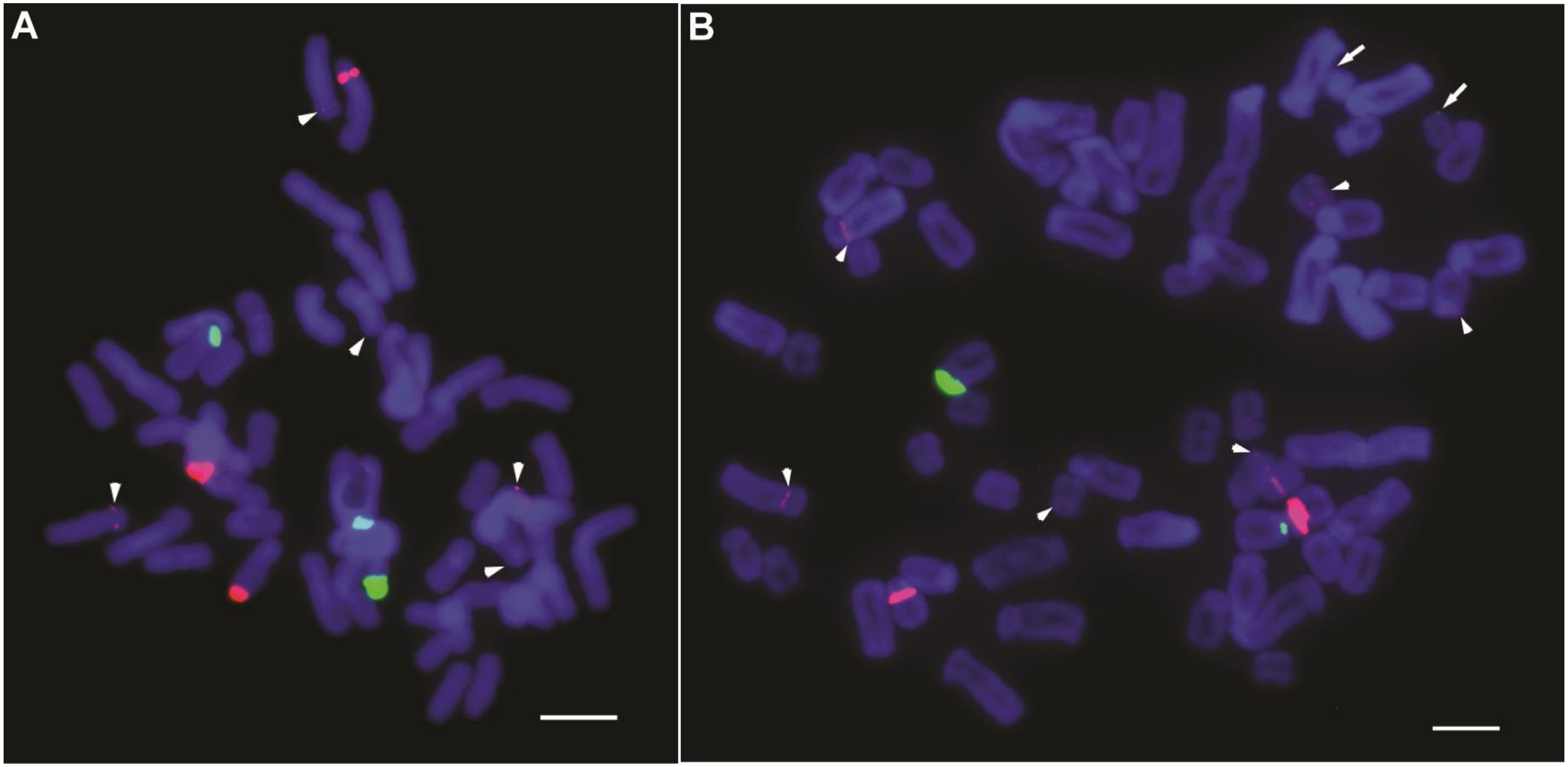

Figure 4-6. Fluorescence in situ hybridization (FISH) on mitotic metaphase chromosomes of (A) *Zephyranthes citrina* (2*n* = 48) and (B) *Sprekelia howardii* (2*n* = 60). Merged images of 5S rDNA (red) and 45S rDNA signals (green) over DAPI stained (blue) chromosomes. White arrowheads indicate weak 5S signals and white arrows denote weak 45S signal. Scale bars = 5 μm.

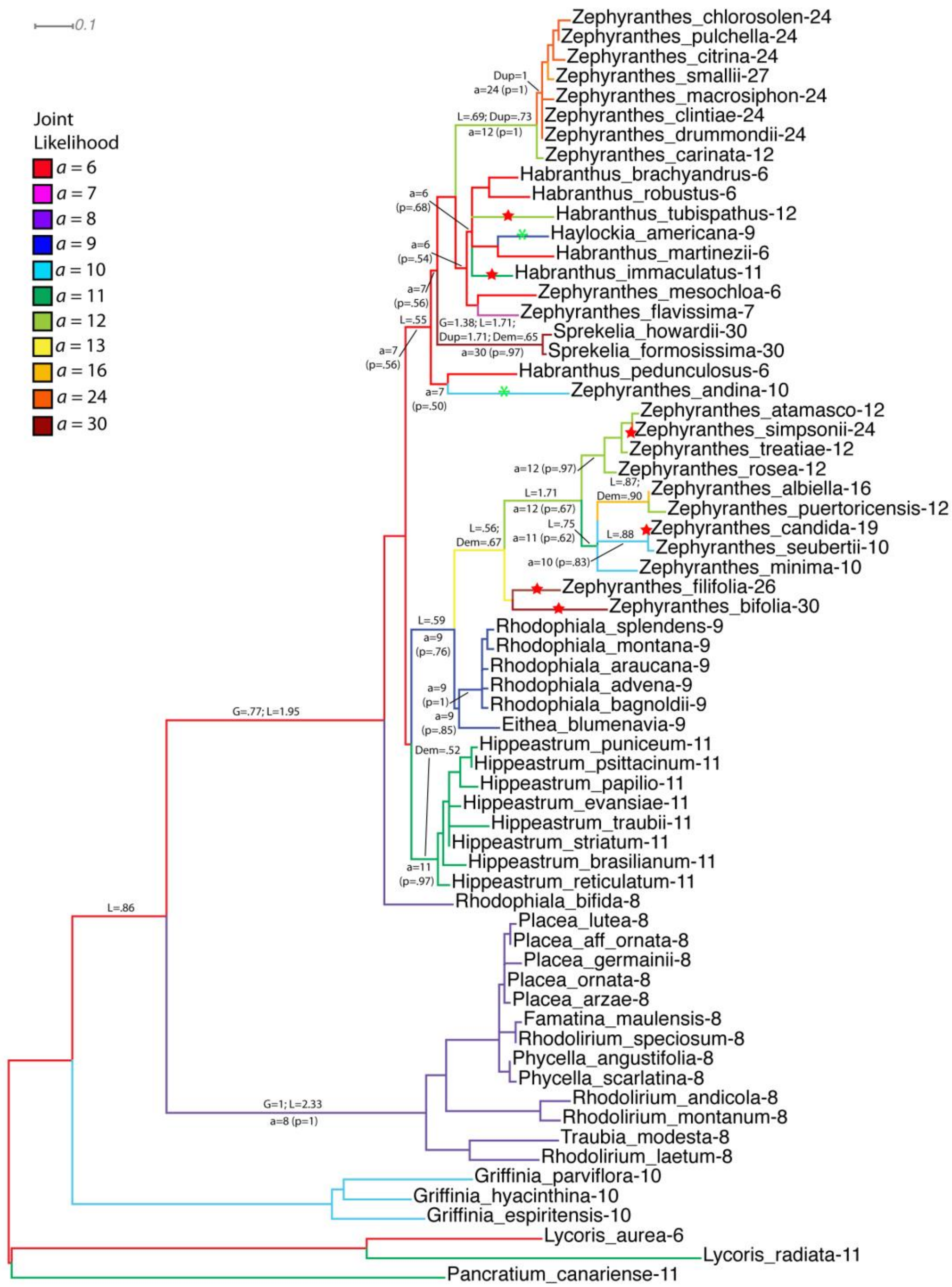

Figure 4-7. Chromosome number evolution inferred over the ITS ML phylogram. Values > 0.5 are shown above branches for chromosome number transitions, and below branches for marginal likelihood of ancestral haploid numbers (*a*). Branches are colored according to the joint likelihood reconstruction of *a*. L: loss; G: gain; Dup: duplication; Demi: demi-duplication; red star: terminal duplication; green asterisk: terminal demi-duplication.

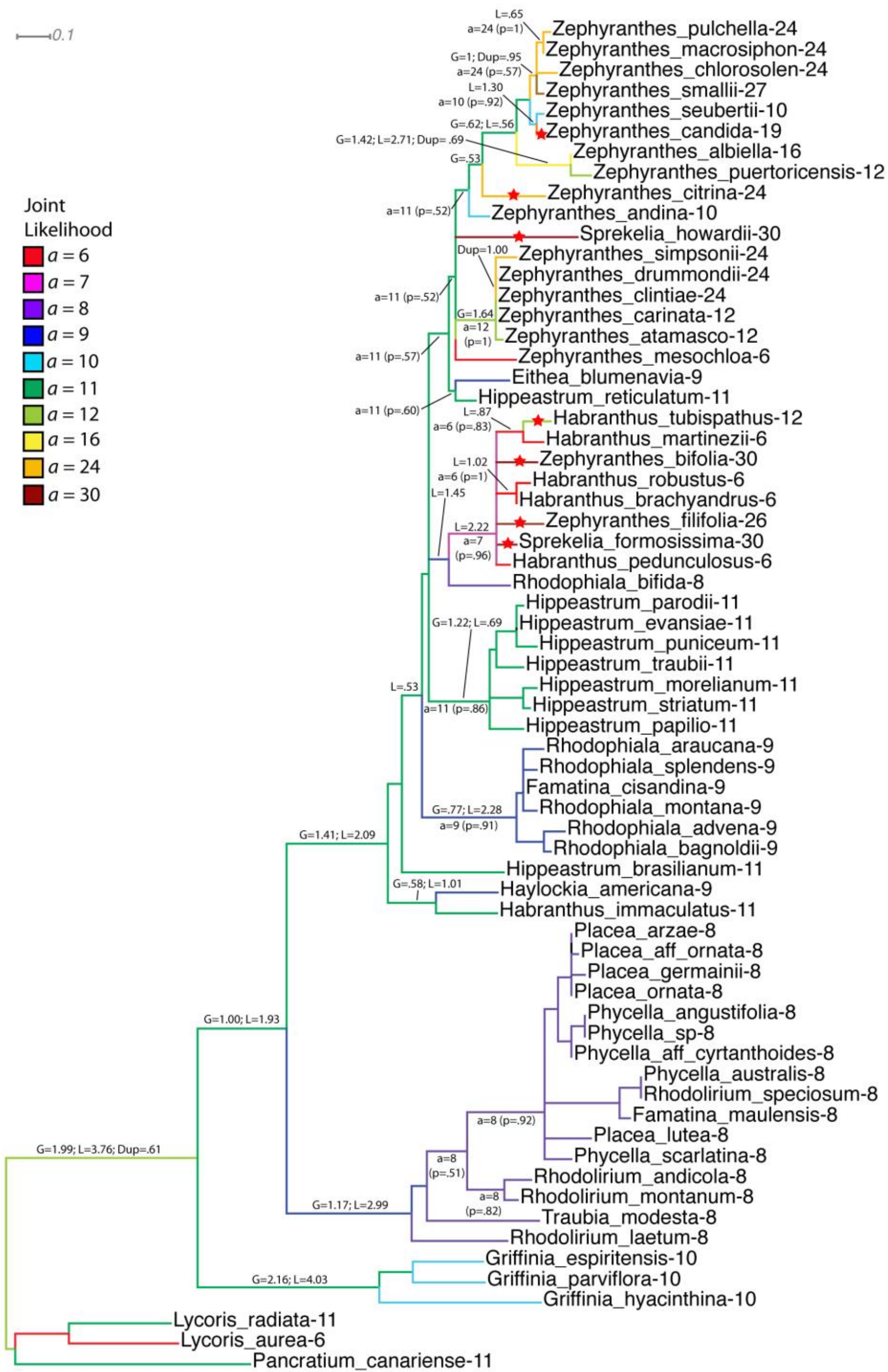

Figure 4-8. Chromosome number evolution inferred over the cpDNA ML phylogram. Values > 0.5 are shown above branches for chromosome number transitions, and below branches for marginal likelihood of ancestral haploid numbers (a). Branches are colored according to the joint likelihood reconstruction of *a*. L: loss; G: gain; Dup: duplication; Demi: demi-duplication; red star: terminal duplication.

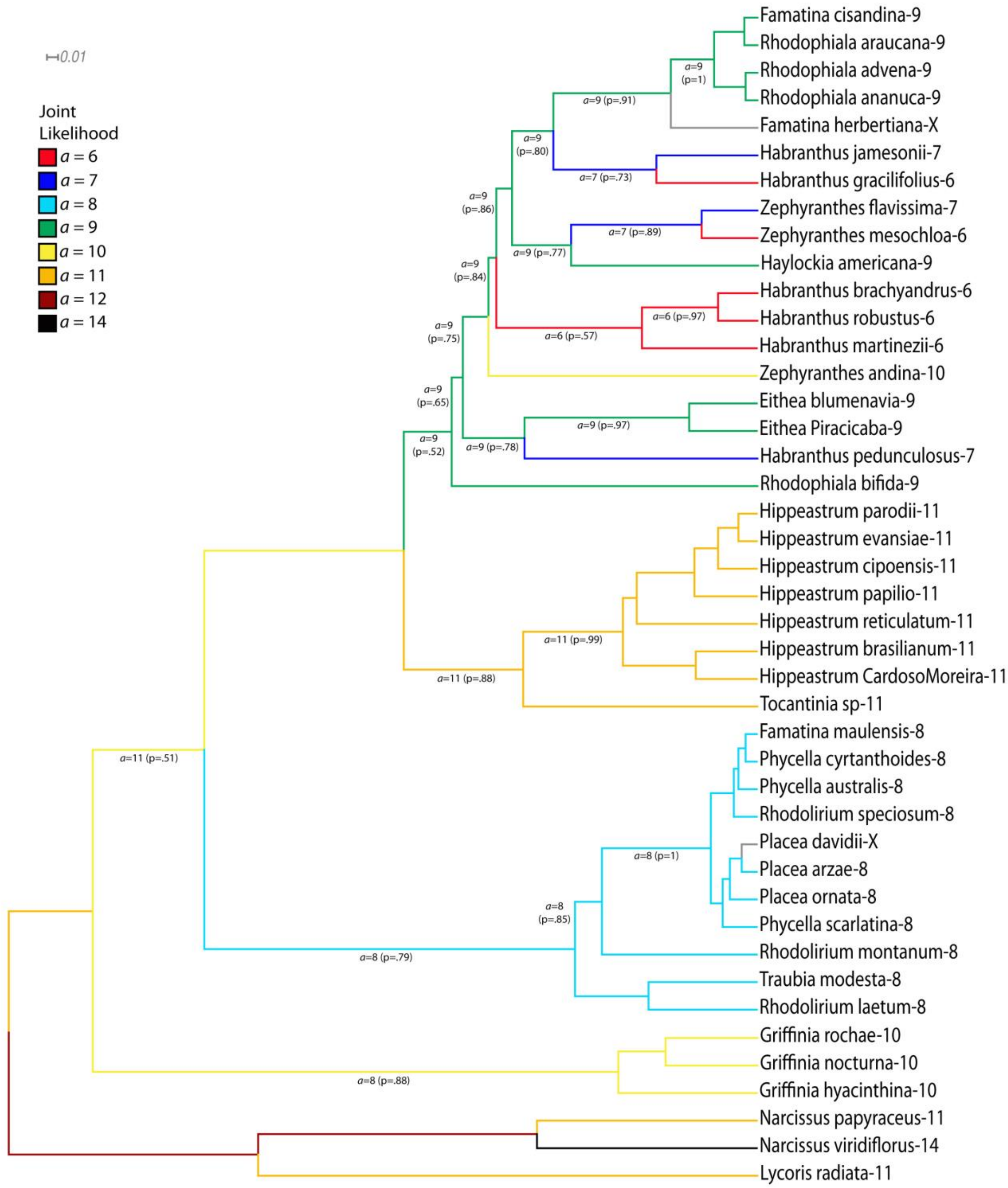

Figure 4-9. Chromosome number evolution inferred over the nuclear (9LCNGs + ITS) species tree for 43 diploid species. Values > 0.5 are shown below branches for marginal likelihood of ancestral haploid numbers (a). Branches are colored according to the joint likelihood reconstruction of *a*.

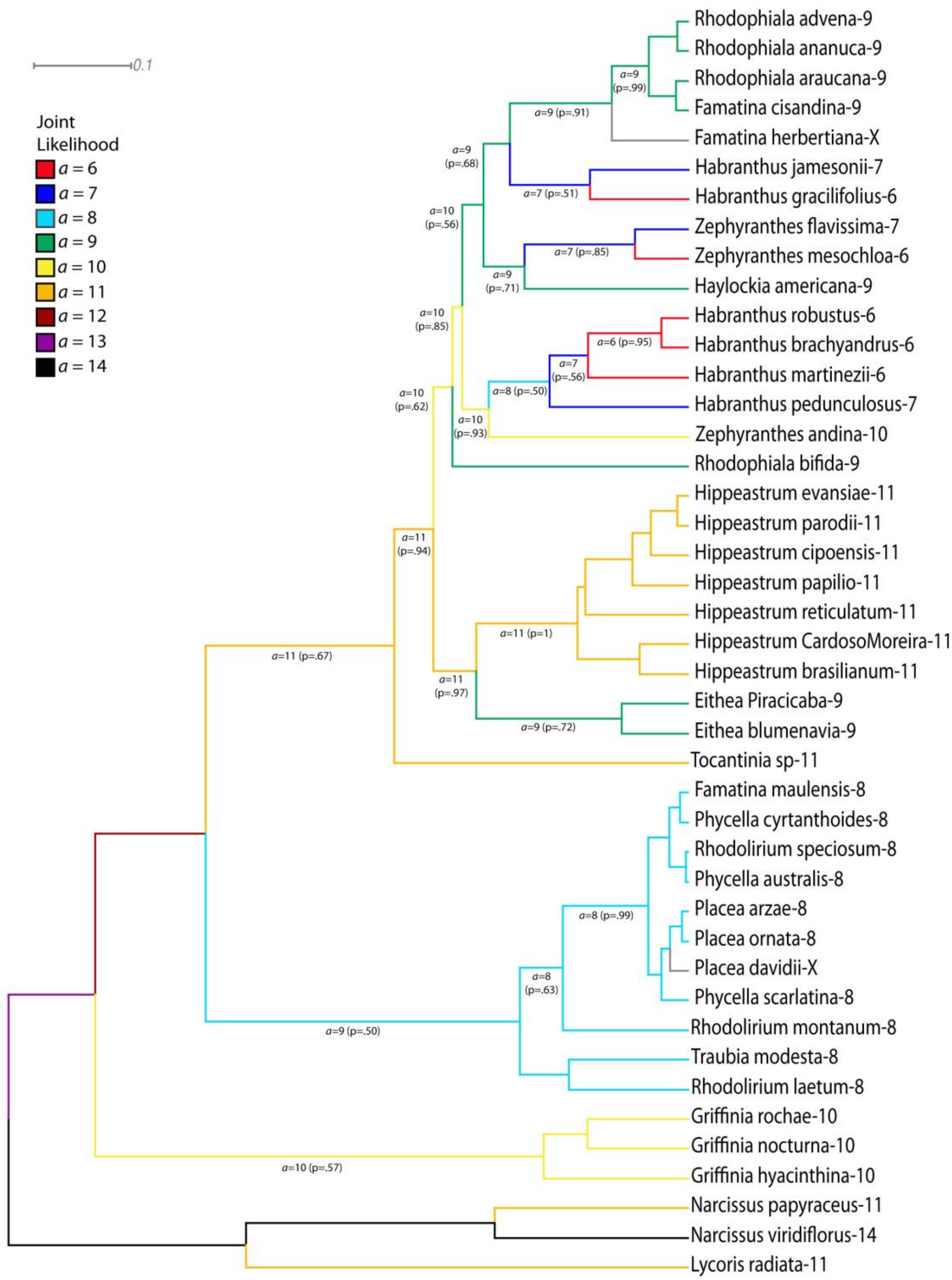

Figure 4-10. Chromosome number evolution inferred over the total (nuclear + cpDNA) species tree for 43 diploid species. Values > 0.5 are shown below branches for marginal likelihood of ancestral haploid numbers (a). Branches are colored according to the joint likelihood reconstruction of *a*.